Earth and Planetary Science Letters 578 (2022) 117320

Contents lists available at ScienceDirect

Earth and Planetary Science Letters

www.elsevier.com/locate/epsl

Calibrating the triple oxygen isotope composition of evaporite minerals as a proxy for marine sulfate

Anna R. Waldeck [a,*,1], Haley C. Olson [a,*,1], Weiqi Yao [e,a], Clara L. Blättler [d], Adina Paytan [b], David A. Hodell [c], David T. Johnston [a]

[a] Department of Earth and Planetary Sciences, Harvard University, 20 Oxford Street, Cambridge, MA 02143, USA
[b] Institute of Marine Sciences, University of California Santa Cruz, 1156 High Street, Santa Cruz, CA 95064, USA
[c] Department of Earth Sciences, University of Cambridge, Downing Street, Cambridge CB2 3EQ, UK
[d] Department of the Geophysical Sciences, University of Chicago, 5734 S. Ellis Avenue, Chicago, IL 60637, USA
[e] Department of Earth Sciences, University of Toronto, 22 Ursula Franklin Street, Toronto, ON, M5S 3B1, Canada

ARTICLE INFO

Article history:
Received 9 April 2021
Received in revised form 6 October 2021
Accepted 25 November 2021
Available online 20 December 2021
Editor: B. Wing

Keywords:
evaporites
barites
$\Delta'^{17}O$
sulfate
seawater
proxy

ABSTRACT

The triple oxygen isotope composition of seawater sulfate, as recorded in marine sulfate evaporites and barites, is commonly used to interpret past changes in atmospheric pO_2/pCO_2 and gross primary production (GPP). In practice, the most-negative measured triple oxygen isotope value ($\Delta'^{17}O$) of sulfate from a marine evaporite deposit is thought to most closely represent contemporaneous seawater sulfate and is used to calculate atmospheric composition. However, a range of triple oxygen isotope compositions are typically measured within a single marine evaporite basin. Here, we characterize in detail the variability in the triple oxygen isotope composition of the sulfate in gypsum sampled from three Messinian (5-6 Ma) marine evaporite sub-basins from the Western Mediterranean Basin. Evaporite sulfate is offset from contemporaneous seawater sulfate and reflects mixing between two end-member sulfate populations: the original seawater sulfate and sulfate that has been isotopically reset after basin restriction. The combined $\Delta'^{17}O$ and $\delta^{18}O$ compositions of sulfate within a stratigraphic context offer the opportunity to better constrain the degree to which marine sulfate evaporites preserve the original isotopic composition of open ocean seawater sulfate. This study encompasses an exploration of mass-dependent fractionation, isotope equilibrium with water, and various scenarios of mixing. Our results calibrate the utility of marine sulfate evaporites in constraining the contemporaneous, open ocean triple oxygen isotope composition of seawater sulfate.

1. Introduction

Atmospheric O_2 is essential to complex multicellular life (Reinhard et al., 2016; Knoll and Sperling, 2014; Knoll, 2011) and a critical component of Earth's surface energy budget (Royer et al., 2007; Berner, 2006). However, no direct records are available that quantify the evolution of the atmosphere, especially O_2, beyond the $\sim 10^6$ yr ice core record (Yan et al., 2019). In recent decades, the triple oxygen isotope ($^{18}O/^{16}O$, $^{17}O/^{16}O$) compositions of sulfate mineral deposits have been suggested to quantitatively reflect the ratio pO_2/pCO_2 in the paleo-atmosphere as well as contemporaneous gross primary production (GPP) (Crockford et al., 2019, 2018; Bao, 2015; Bao et al., 2008). For example, recent work has used this isotope proxy to reconstruct paleo-pO_2/pCO_2 conditions and constrain the timing and tempo of the evolution of oxygenic photosynthesis (Hodgskiss et al., 2019), post-snowball Earth atmospheric conditions (Killingsworth et al., 2013; Bao et al., 2012; Peng et al., 2011; Bao et al., 2009, 2008), and the vigor of primary productivity in the Proterozoic (2500 to 541 Ma) (Crockford et al., 2018). Although promising, much of the mechanistic detail underlying the utility of sulfate minerals to serve as paleoatmospheric records is absent.

Sulfate mineral archives can and do record a wide range of paleo-environments (terrestrial, marine, hydrothermal), each with a unique oxygen isotope life history. Targeting the marine sulfate mineral record in particular provides the most continuity across geological timescales given that seawater integrates a number of global processes and is more buffered from local environmental effects. The stable oxygen isotope composition of seawater sulfate largely reflects a combination of oxidative weathering and microbial recycling (Waldeck et al., 2019). Sulfate primarily enters the

* Corresponding authors.
E-mail addresses: annawaldeck@northwestern.edu (A.R. Waldeck), haleyolson@g.harvard.edu (H.C. Olson).
[1] These authors contributed equally to this work.

https://doi.org/10.1016/j.epsl.2021.117320
0012-821X/

ocean via riverine transport of sulfate derived from evaporite dissolution and/or oxidative weathering of reduced sulfur minerals (e.g. pyrite). Whereas evaporite dissolution contributes sulfate with an inherited oxygen isotope composition, pyrite weathering produces sulfate that has an oxygen isotope composition tied to ambient water, oxygen (O_2), and potentially other sources (Hemingway et al., 2020; Kohl and Bao, 2011; Balci et al., 2007). Once sulfate is in solution (in rivers or the ocean), microbial sulfate reduction in anoxic environments (pore waters, etc.) resets the oxygen isotope composition of marine sulfate (Bertran et al., 2020). The fraction of atmospheric O_2 preserved in marine sulfate depends on initial incorporation during weathering and the vigor of subsequent microbial reworking.

The marine evaporite triple oxygen isotope proxy relies on two main presumptions: (1) the mechanism of oxygen (O_2) incorporation into marine sulfate is understood, and (2) the triple oxygen isotope composition (noted as $\Delta'^{17}O$ and defined in Methods) of seawater sulfate is faithfully preserved in marine sulfate minerals. Work on modern weathering environments (Hemingway et al., 2020) challenges the first of these presumptions. Here, we address the second; specifically, do marine sulfate evaporite deposits record and preserve the oxygen isotopic composition of contemporaneous seawater sulfate?

Marine sulfate evaporite deposits precipitate from restricted marine seawater sulfate reservoirs. However, the extent to which evaporite sulfate is isotopically offset from seawater sulfate composition is less quantitatively understood. Marine evaporite deposits are present throughout the rock record (Evans, 2006; Warren, 2010) and sample a seawater sulfate reservoir that is presumed to be isotopically well-mixed (Waldeck et al., 2019; Johnston et al., 2014). Upon basin restriction from the global ocean, evaporation leads to supersaturation and precipitation of $CaSO_4 \cdot 2H_2O$ (Warren, 2010). In the time after basin restriction, secondary processes such as biogeochemical cycling of sulfur and gypsum dissolution/reprecipitation will overprint the original open ocean sulfate oxygen isotope composition. Alteration away from the seawater sulfate composition is commonplace in these archives, as evidenced by the range of $\delta^{18}O$ and $\Delta'^{17}O$ compositions within any given evaporite unit (Crockford et al., 2019; Claypool et al., 1980). Understanding the extent of this alteration allows for better constraints on the original open ocean sulfate composition.

Here we evaluate the reliability of marine sulfate evaporite minerals to capture the triple oxygen isotope composition of parent seawater sulfate. Central to this exercise is quantifying the isotopic consequences of post enclosure isotope exchange. Here, *post enclosure isotope exchange*, as measured in sulfate, encompasses all processes (biological, chemical and geological) that alter the original open ocean sulfate composition. We report $\Delta'^{17}O$ and $\delta^{18}O$ compositions from Messinian-age gypsum to investigate chemostratigraphic and cross-basinal relationships. We compare these data to contemporaneous marine barite ($BaSO_4$), which is a relatively insoluble mineral that precipitates directly from the open ocean water column (Griffith and Paytan, 2012; Paytan and Griffith, 2007; Bishop, 1988). Marine barite directly constrains the seawater sulfate reservoir composition - from which the Messinian sulfate was originally derived. Collectively, these data allow for quantitative insight and calibration into how the isotopic composition of the Western Mediterranean evaporites were altered away from the open ocean sulfate reservoir. Together, this provides context for interpreting marine sulfate evaporite minerals through time.

2. Geologic setting

The tectonic and glacio-eustatic restriction of the Mediterranean Sea from the Atlantic Ocean defines the Messinian Salinity Crisis (5.96 to 5.33 Ma). This time period is characterized by the cyclical desiccation and flooding of the Mediterranean Basin and the deposition of evaporite parasequences (Hsü et al., 1973; Krijgsman et al., 1999; Gargani and Rigollet, 2007). Gypsum ($CaSO_4 \cdot 2H_2O$) is a major mineral constituent in these sequences and represents the primary sulfate-bearing mineral phase that was deposited during basin evaporation. The deposits are defined by a period of evaporation (marked by gypsum and evaporite salts) interrupted by freshening (marked by carbonate marls). The isotopic composition of hydration water and salinity of gypsum fluid inclusions from the Sorbas Basin, a Western Mediterranean sub-basin, suggest that the chemostratigraphic variability observed in the sequences is due to low-temperature biogeochemical or physical processes and not to significant post-burial heat or pressure-induced alteration. Thus, these sequences, and other sequences in similar basins, are ideal targets for assessing secondary isotope exchange processes (Evans et al., 2015).

Evaporite samples were collected from three sub-basins across the broader Western Mediterranean Basin: the Yesares Member in the Sorbas Basin, Spain; the Monte Grotticelle Formation in the Caltanissetta Basin, Sicily; and Ocean Drilling Project (DSDP) Leg 107, Site 654, Hole A, located off the coast of Sardinia in the Tyrrhenian Basin (Figure S1). Herein, we use the sub-basin names to refer to each set of evaporite sequences. It has been suggested that the on-shore Caltanissetta and Sorbas Basin sections are correlative across the Western Mediterranean Basin and are both part of the Primary Lower Gypsum facies (Stefano et al., 2010; Roveri et al., 2014). The base of both units is dated to ~5.9 Ma using a chronostratigraphic astronomical tuning model (Krijgsman et al., 2001). The lowermost sequences captured by Hole 654A are slightly younger, dated at ~5.5 Ma (Roveri et al., 2014).

For comparison to the Messinian evaporites, we include the characterization of marine barite (n = 5) extracted from a sediment core at Ocean Drilling Program Site 849, Hole 849D, located in the eastern equatorial Pacific (at 0°10.993'N, 110°31.167'W (Mayer et al., 1992)). These samples were dated to 6.9 Ma to 4.3 Ma following the Geological Time Scale 2020 (Gradstein et al., 2020) using the Neptune database (Renaudie et al., 2020; Lazarus, 1994; Spencer-Cervato, 1999). These marine barites provide a critical constraint on open ocean seawater at the time of the Messinian Salinity Crisis.

3. Chemical methods

Evaporite samples required purification and conversion to barium sulfate, the phase used in isotopic analyses. For each sample, ~100 mg of powdered, homogenized evaporite was dissolved in weak HCl (0.1 mM, 125 mL) on a shaker table at 60 °C overnight. The dissolved sulfate was isolated via chromatography (Le Gendre et al., 2017). Empty polypropylene SPE tubes with 20 mL volume were packed with 5 g of AG1-X8 anion exchange resin and preconditioned with 3x20 mL of 3 M HCl followed by 3x20 mL of deionized (DI) water. Dissolved SO_4^{2-} solutions were loaded onto columns at a rate of 1 mL/min, and subsequently eluted with 44 mL of 0.4 M HCl. To quantitatively precipitate $BaSO_4$, 1-2 mL of 1 M $BaCl_2$ solution was added. Samples were then centrifuged, rinsed 3 times with DI, and dried in a 60 °C oven.

Marine barite samples were handled differently. Barite was first extracted from sediments following a sequential dissolution method (Paytan et al., 1993; Markovic et al., 2016) and further cleaned by dissolution in sodium carbonate (Breit et al., 1985; Von Allmen et al., 2010; Markovic et al., 2016). Following sequential leaching and extraction of barite from sediments, the remaining barite was collected onto filter paper and heated at 750 °C in the furnace for 1 h to oxidize highly refractory organic matter. Afterwards, samples were weighed and added to PTFE vials with a 0.5 M Na_2CO_3 solution in a ratio of 10 mg $BaSO_4$ to 2 mL of

Na_2CO_3 solution. The sample mixtures were sonicated at room temperature for 60 min and then placed in an 80 °C oven for 16 h. The sodium carbonate step was performed three times. After the third collection, barium chloride was added (10% $BaCl_2$ in 2 M HCl) until samples reached pH<2, to precipitate $BaSO_4$. Samples were rinsed 2 times in 2 N HCl, 3 times in DI, and dried at 60 °C.

Purified barite was then subjected to two different forms of isotope analyses. First, for $\delta^{18}O$ analysis, ~250±50 μg of clean dry barite was weighed in triplicate into silver capsules (Elemental Microanalysis; 4x3.2 mm) with AgCl and glassy C additive in an approximately 2:1 mass ratio. Before measurement, weighed sample capsules were dried at 60 °C in a vacuum oven overnight. All samples were run using a high-temperature conversion elemental analyzer (TC/EA) connected to a Thermo Scientific Delta V Plus isotope ratio mass spectrometer configured in a continuous flow mode. The $\delta^{18}O$ data were corrected to accepted values for IAEA-SO5, IAEA-SO6, and NBS-127 (Brand et al., 2009). Samples were corrected for the amount of additive, drift over the course of the analysis, and scale compression. All isotope ratios are reported in units of ‰, following:

$$\delta^{18}O_{\text{sample}} = 10^3 * \left(\frac{{}^{18}R_{\text{sample}}}{{}^{18}R_{\text{standard}}} - 1 \right). \quad (1)$$

The long-term reproducibility (1 σ) of standards is <0.6‰ (n = 282).

For minor oxygen isotope analyses, barite was measured according to published protocols (Cowie and Johnston, 2016). Here, approximately 5 mg of purified $BaSO_4$ was reacted in a pure F_2 atmosphere by heating with a 50 W CO_2-laser, which liberates O_2 along with other fluorinated byproducts. Sample gas was passed through multiple cryo-focus steps and an in-line gas chromatograph before being introduced as pure O_2 to a Thermo Scientific MAT 253 gas source isotope ratio mass spectrometer configured in dual-inlet mode. Each $\delta^{18}O$ and $\delta^{17}O$ were taken as the mean of 4 acquisitions of 10 cycles with a target of 3000-5000 mV on the m/z 34-cup. The measured $\delta^{17}O$ and $\delta^{18}O$ values were subsequently corrected to a least squares regression through the triple oxygen isotope composition of air and the IAEA silicate standards UWG-2 and NBS-28 (Wostbrock et al., 2020) corrected to a VSMOW/SLAP scale (see SOM for further discussion). The corrected $\Delta'^{17}O$ for each sample, defined as:

$$\Delta'^{17}O_{\text{sample}} = 10^3 * \left(\ln\left(\frac{\delta^{17}O_{\text{sample}}}{1000} + 1 \right) - \theta_{\text{RF}} * \ln\left(\frac{\delta^{18}O_{\text{sample}}}{1000} + 1 \right) \right) \quad (2)$$

where θ_{RF} is the slope of the mass dependent reference line, herein we use $\theta_{\text{RF}} = 0.5305$. Using a set of internal standards, we report a precision on sulfate of 0.02‰ for $\Delta'^{17}O$. All $\Delta'^{17}O$ data is presented on the silicate-derived VSMOW/SLAP scale along with the true TC/EA-derived $\delta^{18}O$ value (Wostbrock et al., 2020).

4. Results

The sampled evaporites are from three stratigraphic sections spanning the Western Mediterranean Basin: (A) Sorbas Basin (n = 38), (B) Tyrrhenian Basin (n = 13), and (C) Caltanissetta Basin (n = 11) (see Figure S1). Samples from the Sorbas Basin have an average measured $\delta^{18}O$ of 12.9±1.1‰ and an average $\Delta'^{17}O$ = −0.012±0.033‰. The Tyrrhenian Basin has an average $\delta^{18}O$ = 17.3±1.6‰ and $\Delta'^{17}O$ = −0.023±0.023‰. The Caltanissetta Basin has an average $\delta^{18}O$ = 14.2±0.7‰ and $\Delta'^{17}O$ = −0.037±0.020‰. Data from each of these basins are normally distributed for both $\delta^{18}O$ and $\Delta'^{17}O$, and for the most part there are no resolvable chemostratigraphic trends (see SOM for exceptions). According to a student's t-test, all three basins have distinct populations of $\delta^{18}O$ values. The Caltanissetta and Tyrrhenian Basins have $\Delta'^{17}O$ distributions that are statistically indistinguishable from each other, but distinct from the Sorbas $\Delta'^{17}O$ distribution.

Barite data comes from modern core tops (for calibration) and Messinian (7.2 to 5.3 million years ago) and Zanclean (5.3 to 3.6 million years ago) marine sediments. Consistent with previous work (Markovic et al., 2016), we find a small offset in coretop barite $\delta^{18}O$ = 6.2±0.6‰ (n = 4, this study) from modern seawater sulfate $\delta^{18}O$ = 8.7±0.2‰ (n = 178 (Johnston et al., 2014)). The coretop barite $\Delta'^{17}O$ = +0.033±0.009 (n = 3, this study) is statistically indistinguishable from the modern seawater sulfate composition $\Delta'^{17}O$ = +0.037±0.016[2] (n = 24 (Waldeck et al., 2019)). The Messinian-aged barite samples (n = 5, Ocean Drilling Program Hole 849D) have a $\Delta'^{17}O$ composition with an average value of +0.015±0.029‰ and a $\delta^{18}O$ composition of 7.1±0.3‰.

5. Discussion

To date, interpretations of the triple oxygen isotope composition of the sulfate evaporite record have centered on its use as a proxy for contemporaneous tropospheric oxygen (Crockford et al., 2019). However, there exist a number of different physical and biogeochemical processes that together set the oxygen isotope composition of sulfate evaporite minerals; this complicates quantitative linkages to paleoatmospheric compositions. In practice, Earth scientists logically use the most negative measured sulfate evaporite $\Delta'^{17}O$ value as a measure of the least-altered, best-estimate of contemporaneous seawater (or terrestrial) sulfate (Crockford et al., 2019, 2018; Bao et al., 2008). In this work, we look to extend the utility of that approach. We ask how basinal alteration affects triple oxygen isotope compositions and how we might extract additional information from ancient evaporite populations, rather than simply relying on the most negative $\Delta'^{17}O$.

5.1. Messinian evaporite as an environmental record

We use the relatively young, well-studied, and heavily-sampled sulfate evaporites from the Messinian Western Mediterranean Basin as a case study to explore the effects of post enclosure isotope exchange processes on the oxygen isotope composition of marine evaporite. The term *post enclosure isotope exchange* here encompasses all processes that alter the isotope composition of sulfate once the evaporite basin is separated from the open ocean.[3] We compare our data to Messinian seawater sulfate composition derived from the marine barite mineral record and use this isotopic offset to calibrate the extent of post enclosure isotope exchange. The degree to which post enclosure isotope exchange affects the sulfate isotope composition depends on many factors. As examples, marine evaporite basins may differ in degree of basin restriction, water exchange, meteoric water inputs, evaporation, and evaporite mineral precipitation kinetics, before even considering local biogeochemistry. Even in our well-constrained case study, we do not have all of the tools to uniquely disentangle the complex evaporite basin sulfur cycle. However, we can most simply interpret the Messinian Western Mediterranean Basin evaporite sulfate isotope composition as comprising two components: (1) initial contempo-

[2] This seawater composition reflects the data from Waldeck et al. (2019) with an updated and improved three point correction scheme to VSMOW/SLAP scale, see SOM for full details.

[3] At the same time, varying degrees of restriction and episodic connectivity to the open ocean are likely over the lifetimes of these marine evaporite basins.

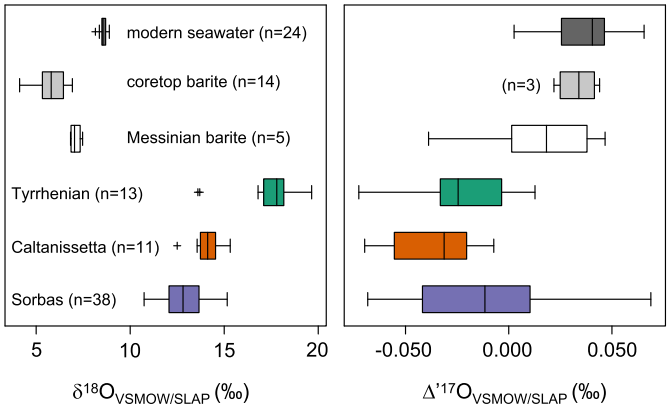

Fig. 1. Box and whisker plots of sulfate for each sample population. The left panel displays the $\delta^{18}O$ distributions, and the right panel $\Delta'^{17}O$. The sample population size (n) is also included. The boxes span the 25^{th} to 75^{th} percentiles and include a vertical line for the median $\delta^{18}O$ or $\Delta'^{17}O$ value.

raneous seawater sulfate and (2) sulfate that has been overprinted by post enclosure isotope exchange processes.

5.2. Marine barite constraints on seawater sulfate

Marine barite collected from seafloor sediments is a powerful and widely used proxy for ancient seawater sulfate (Paytan et al., 1998, 2004; Turchyn and Schrag, 2004, 2006; Johnston et al., 2014). Thus, Messinian marine barite ($BaSO_4$) is used to estimate the isotopic composition of open ocean seawater sulfate during the Messinian Salinity Crisis. Previous work on oxygen isotopes in marine barite suggests a small offset in the $\delta^{18}O$ of barite relative to seawater sulfate (2-3‰ (Markovic et al., 2016)). Our new modern coretop barite data are consistent with such an offset. Paired with the published literature (Markovic et al., 2016), we find a mean barite offset of 2.7±0.6‰ (n = 14) toward lower $\delta^{18}O$ relative to water column sulfate (Markovic et al., 2016; Johnston et al., 2014). We extend these traditional applications to ^{17}O, where we do not observe a statistically distinguishable offset in barite $\Delta'^{17}O$ relative to water column sulfate (Waldeck et al., 2019) (Fig. 1). Given the relatively small $\delta^{18}O$ offset, the unresolvable $\Delta'^{17}O$ offset is expected.

We next determine the oxygen isotope composition of seawater sulfate during the time of Messinian evaporite deposition (from 5.9 to 5.3 Ma (Krijgsman et al., 1999)). Late Miocene (Messinian) and early Pliocene (Zanclean) barite ranging in age from 6.9 to 4.3 Ma were targeted (n = 5, Ocean Drilling Program Hole 849D) - this time window was selected based on the age of Messinian evaporites and a ~ ±1 Ma residence time of oxygen in seawater sulfate (Turchyn and Schrag, 2004, 2006). These barites have a mean $\delta^{18}O$ = 7.1±0.3‰ and $\Delta'^{17}O$ = 0.015±0.029‰. Given the offsets noted above, we predict $\delta^{18}O$ of late Miocene seawater sulfate was likely within 9.8±0.9‰ with a $\Delta'^{17}O$ equivalent to that noted above (Fig. 1). We use this seawater sulfate composition as the best estimate of the sulfate in the Mediterranean Basin prior to enclosure (one of the end-members in our mixing model).

5.3. Constraints on post enclosure isotope exchange

A comparison between the estimate of late Miocene seawater sulfate $\delta^{18}O$ and $\Delta'^{17}O$ and the three sampled Mediterranean sub-basin evaporites demonstrates how the composition of basinal sulfate can differ from the originally adopted, open marine sulfate signal. As has been previously documented (Palmer et al., 2004; Utrilla et al., 1992), and illustrated in Figs. 1-3, the $\delta^{18}O$ of marine sulfate evaporite minerals is enriched relative to that of seawater sulfate. The enrichment in ^{18}O is likely driven by basinal sulfate recycling, which can be generically attributed to a couple different

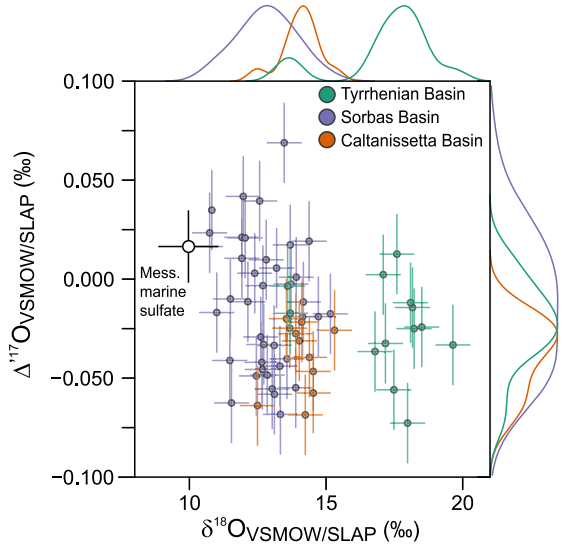

Fig. 2. Evaporite $\Delta'^{17}O$ and $\delta^{18}O$ data from the Sorbas, Tyrrhenian, and Caltanissetta Basins with 1σ reflecting analytical uncertainty. Corresponding kernel density estimates for each locality are plotted on the figures outer edge. All data are reported on a VSMOW/SLAP scale.

scenarios. First, if isotopically depleted sulfate is removed from the system (for instance, during kinetically driven sulfate reduction), the $\delta^{18}O$ of the residual sulfate increases (consider Rayleigh fractionation/distillation). However, evidence for a large sulfate reduction flux is lacking (the overwhelming majority of the stratigraphy is composed of gypsum). As a second and more likely scenario, in the case of a sulfate-rich evaporite basin, we expect that sulfate exchanges O atoms with H_2O as it is biogeochemically cycled (Bertran et al., 2020; Turchyn et al., 2006; Brunner et al., 2005; Fritz et al., 1989). For example, partial reduction of sulfate to lower valence state S and subsequent re-oxidation to sulfate (whether microbially or inorganically mediated) resets the isotopic composition of that product sulfate (more below). Along with $\delta^{18}O$, the basinal distributions of $\Delta'^{17}O$ are similarly offset (by an average of ~0.04‰ across all three sub-basins) to lower values relative to contemporaneous seawater sulfate. In the case of the Messinian, marine evaporite sulfates with lower $\delta^{18}O$ and higher $\Delta'^{17}O$ values are thus most reflective of the starting seawater sulfate composition. In other words, the Sorbas Basin is most closely related to seawater sulfate while the Tyrrhenian Basin is most isotopically evolved. Though developed using the Messinian Western Mediterranean Basin, this framework should apply to marine evaporite basins more generally. The initial composition of dissolved sulfate

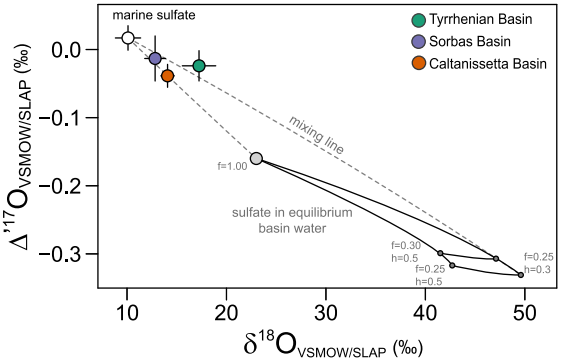

Fig. 3. The triple oxygen isotope composition of sulfate in each sub-basin (colored circles) is plotted with a barite-derived estimate for late Miocene seawater sulfate (white circle). Dashed lines extend from Messinian-age seawater sulfate (white circle) to the calculated isotopic composition of fully equilibrated sulfate if basinal waters carry an oxygen isotope composition equal to that of the modern ocean (gray circle). The triangular region in the bottom right encompasses a range of possible fully equilibrated sulfate oxygen isotope compositions that reflect the effect of evaporative fractionation of seawater. Solid lines indicate the potential range of relative humidity values (h) and extent of evaporation (f, as the fraction of the reservoir remaining) used to calculate the fractionation of water oxygen isotopes (following Passey and Levin (2021); see SOM for further discussion). (For interpretation of the colors in the figure(s), the reader is referred to the web version of this article.)

should evolve toward a sulfate equilibrium end-member, with $\delta^{18}O$ and $\Delta'^{17}O$ tied to that of environmental water.

The direction of this combined offset (higher $\delta^{18}O$ and lower $\Delta'^{17}O$) is consistent with thermodynamic and kinetic principles. The vast majority of low-temperature biogeochemical and physical processes are mass-dependent, which enrich the ^{18}O composition of sulfate and deplete the ^{17}O composition. The isotope nomenclature used to quantify mass-dependence, referred to as θ, defines the slope of this relationship. The decrease in $\Delta'^{17}O$ as $\delta^{18}O$ increases is also in part a function of $\theta_{RF} = 0.5305$ (Equation (2)), and the fact that mass-dependent processes (biology, inorganic equilibrium, etc.) have associated θ values that are less than this reference value ($<$0.5305). When tethered to Messinian open ocean sulfate and interpreted most simply, the Sorbas Basin falls along $\theta \approx 0.521$, the Caltanissetta Basin along $\theta \approx 0.518$, and the Tyrrhenian along $\theta \approx 0.525$. The mixing array connecting open ocean seawater sulfate and sulfate equilibrated with seawater (Fig. 3) is captured by and apparent θ ranging from 0.518 to 0.521. Note that this slope is a representation of mixing, not the mass law for sulfate-water equilibrium. This leaves two possible explanations. The first, and less likely, is that different physical processes with different intrinsic θ values are altering each sub-basin independently. Instead, these differing arrays likely reflect variable equilibration with basinal water, but that basinal water has itself evolved away from seawater.

We view the oxygen isotopic evolution of basinal sulfate as driven by processes that equilibrate sulfate with ambient H_2O. For example, during microbial sulfate reduction, incomplete reduction generates an efflux of cellular sulfate that largely reflects an isotopic equilibrium between intermediate valence sulfite and cellular water (Bertran et al., 2020; Turchyn and Schrag, 2006; Brunner et al., 2005; Fritz et al., 1989). By extension, this requires predictions for the evolution of the oxygen isotope composition of basinal water. During initial restriction of the Mediterranean, basin water reflected seawater composition (likely around $\delta^{18}O_{H_2O} = 0‰$ and $\Delta'^{17}O_{H_2O} = 0‰$, e.g. Grossman and Joachimski (2020)). Excess evaporation (3-4x by volume) is required to reach gypsum saturation, and this process increases the $\delta^{18}O$ and decreases the $\Delta'^{17}O$ of basinal waters (Passey and Levin, 2021). Meteoric inputs can counteract these effects, contributing water with lower $\delta^{18}O$ and higher $\Delta'^{17}O$ (Sharp et al., 2018). A study of gypsum hydration waters predicts that Western Mediterranean Basin waters are a mixture of evolved water (altered by evaporation) and meteoric water, yielding triple oxygen isotope composition around $\delta^{18}O_{H_2O} = 0‰$ and $\Delta'^{17}O_{H_2O} = 0‰$ (Evans et al., 2015). Sulfate equilibrium would then be offset from water by roughly 23‰ for $\delta^{18}O$ and $-0.148‰$ for $\Delta'^{17}O$ at 25 °C (Zeebe, 2010; Cao and Bao, 2021). The triangular region at bottom right in Fig. 3 encompasses the possible oxygen isotope compositions of equilibrated sulfate, depending on the ambient basin water composition. We consider variable degrees of evaporation (f=the fraction of initial volume remaining) along with plausible relative humidities (h; Fig. 3; following (Passey and Levin, 2021), see SOM for further details) to further define this approach.

The context provided above, where basinal waters may be variable and isotopic alteration within a basin is related to sulfate-water isotope equilibrium, satisfies a majority of the observations. As presented in Fig. 3, both the Sorbas and Caltanissetta Basins fall along a line related to nearly unaltered seawater, with a small degree of secondary re-equilibration (the distance along the mixing line). The more evolved Tyrrhenian Basin falls slightly outside this field. As there are mixing solutions that can satisfy all three sub-basins (at the 2σ level), we stop short of invoking some alternative process or life history as being responsible for the composition of the Tyrrhenian Basin. That said, as more is known about process-specific, triple oxygen isotope mass laws, this presumption should be revisited.

5.4. Isotopic variability within evaporitic basins

With a growing understanding of the nature of the offset captured in the Messinian evaporite $\delta^{18}O$ and $\Delta'^{17}O$ records, we look to extend the interpretability of evaporite datasets more generally. The Messinian dataset is handled as three discrete populations (per sub-basin). Each sub-basin (Sorbas ($n = 38$), Caltanissetta ($n = 11$), and Tyrrhenian ($n = 14$)) has a distribution of $\delta^{18}O$ and $\Delta'^{17}O$ compositions that are Gaussian, or "normal" (i.e. pass a Shapiro-Wilk test with a standard p-value threshold of 0.05 - this test is used throughout for normality). We note that the confidence in a normality test depends largely on the size of the datasets. For example, a dataset of size n = 6 that passes the S-W normality test could theoretically derive from a normal, Poisson, uniform, or an exponential distribution (Razali et al., 2011) (the connection between sampling density n and variability in distribution shape is explored in the SOM and should be considered when interpreting geological datasets). The normalities of the Messinian sub-basin data distributions imply that the sulfate reservoir from which gypsum precipitated was well-mixed. More specifically, we infer that the Western Mediterranean Basin was homogeneous with respect to sulfate oxygen isotope compositions over the integrated time of evaporite deposition captured within our sampled stratigraphy.

While we interpret the evaporite basin as approximately well-mixed at any given time, we also observe long-term isotopic evolution within the basin. The most apparent difference is the higher sulfate $\delta^{18}O$ composition in the ≈300 kyr younger Tyrrhenian Basin, relative to the other two sub-basins.[4] The Sorbas and Caltanissetta evaporites are similar in age; a comparison of sulfate from correlated cycles (3-6) between the two localities is indistinguishable based on the overlapping 1σ of the mean $\delta^{18}O$ and $\Delta'^{17}O$ from each sub-basin. That said, the uniqueness of the three $\Delta'^{17}O$ sub-basin distributions is dependent on how the measurements are grouped. The Caltanissetta and the Sorbas Basin cycles 3-6 have statistically indistinguishable $\Delta'^{17}O$ distributions. How-

[4] We confirm that the Tyrrhenian sample $\delta^{18}O$ distribution is distinct from the other two sub-basins using a student's t-test.

ever, gypsum from cycles 1, 2, and 7 in the Sorbas Basin contributes higher $\Delta'^{17}O$ and lower $\delta^{18}O$ compositions. When fully grouped, the Sorbas Basin population is then distinct in both $\delta^{18}O$ and $\Delta'^{17}O$ from the two other sub-basins. These differences between evaporitic cycles may reflect real changes in basin sulfur cycling and/or an evolving isotopic composition of basinal water. Importantly, this interpretation is possible given tight stratigraphic context and an age model.

The sort of mixing relationships noted above - between original seawater sulfate and that which has been reset in the basin - can be modeled in a couple of different ways. Here we attempt to additionally use the distribution and form of the resulting "mixed" data as a guide. The first approach, which we term *additive* mixing, is drawn from statistical theory and makes specific predictions for the distribution of data as mixing progresses. The second approach, termed *homogeneous* mixing, leans more heavily on the observation that each of the Western Mediterranean sub-basins are normally distributed. For both, we use our approximation for open ocean Messinian seawater sulfate ($\delta^{18}O = 9.8\pm0.9$‰ and $\Delta'^{17}O = +0.015\pm0.029$‰) as the initial end-member. As discussed above, the second end-member can vary between basins or across time. For this exercise, we presume a normally distributed population of sulfate $\delta^{18}O$ and $\Delta'^{17}O$ that is tethered to a predicted H_2O composition via an equilibrium isotope effect. We assign the basin-/time-specific end-member a distribution rather than a single value in order to account for environmental and analytical uncertainties that would accompany the description of this end-member, had it been possible to be uniquely identified and measured.

We begin with our *additive* mixing scheme. Here, theory dictates that a normal distribution is described by its probability density function (PDF) using the expression:

$$g(x, \mu, \sigma^2) = \frac{1}{\sigma\sqrt{2\pi}} e^{\frac{-(x-\mu)^2}{2\sigma^2}}, \tag{3}$$

where x is an independent variable, μ is the mean and σ is the standard deviation of each distribution. As an extension of this, the mixture of two normal distributions (or sulfate sources), is written as:

$$g(x, \mu_{p1}, \sigma_{p1}^2, \mu_{p2}, \sigma_{p2}^2) = \frac{f_{p1}}{\sigma_{p1}\sqrt{2\pi}} e^{\frac{-(x-\mu_{p1})^2}{2\sigma_{p1}^2}} + \frac{f_{p2}}{\sigma_{p2}\sqrt{2\pi}} e^{\frac{-(x-\mu_{p2})^2}{2\sigma_{p2}^2}}, \tag{4}$$

where f_p is the fractional contribution of each source, and where $f_{p1} + f_{p2} = 1$. If the mean value of population 1 (p_1, or the original open ocean seawater sulfate) is mixed with that of population 2 (p_2, or the reset sulfate), the product is a new mean that reflects the proportional mixture. This can be written as a common numerical isotope mass balance calculation (like f_{org}, f_{py}, etc) of the form:

$$\mu_3 = f_{p1} \cdot \mu_1 + (1 - f_{p1}) \cdot \mu_2, \tag{5}$$

where the mean (μ_3 of the new population, p_3) is a weighted sum of the means of the inputs, μ_{p1} and μ_{p2}, from distributions p_1 and p_2. However, this simple logic misses additional features of the distributions that, by definition, tell us something about the system and are worth exploration. Recall that our sub-basins are normally distributed in both $\delta^{18}O$ and $\Delta'^{17}O$. The expression above (Eqn. (4)) yields a bimodal probability density function during mixing (rather than a single normal population), with each mode representing the mean of p_1 and p_2 distributions (see Fig. 4). When mixing, this model keeps contributions from p_1 and p_2 separate. This would be analogous to sampling Messinian gypsum and uniquely diagnosing which sulfate molecules derive from

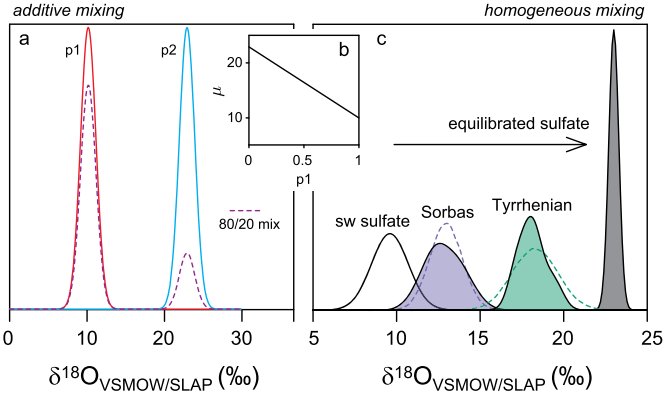

Fig. 4. The two mixing models are compared, with additive mixing illustrated in frame a and homogeneous mixing in frame c. In frame a, two populations p1 and p2 are mixed together, resulting in the 80/20 mixture reflected by the dashed line. In panel c, the two end-member populations are seawater sulfate and equilibrated sulfate; homogeneous mixing of different proportions results in the dashed lines that roughly approximate the actual Sorbas and Tyrrhenian PDFs (filled purple and green areas). Frame b depicts the changing mean value μ as mixing proceeds (here denoted as the fractional contribution from p1, from 0 to 1). While the trajectory of the mean value for both mixing models is the same, the shapes of the distributions differ.

original seawater sulfate (p_1) and which were via 'post basin isotope exchange' processes (p_2). This is not what is recorded in the Messinian sub-basins - a conclusion that is supported when other features of the predicted mixture data distribution output (like skew and kurtosis) are considered. Although not our preferred solution, but for completeness, we provide a full derivation of how *additive* mixing affects the features of a data population (the mean, variance, skew and kurtosis) in the SOM.

Next we consider what we term a *homogeneous* mixing of two end-member populations. Rather than keeping separate the contributions from each end-member population, the mixed population is composed of individual values that are themselves weighted averages. Each individual value x_3 in the mixed population is itself derived from individual values x_1 and x_2 from the two end-member populations, following: $x_3 = f_{p1} \cdot x_1 + f_{p2} \cdot x_2$. This model results in a well-mixed, normally distributed population, p_3, with a mean isotope composition that similarly reflects the weighted average of the two end-member μ values (Equation (5)). In Fig. 4, homogeneous mixing then predicts that Sorbas Basin sulfate has a composition closer to the starting seawater sulfate (x_1) than the Tyrrhenian Basin sulfate. The mechanism behind the difference in the isotopic composition of the Tyrrhenian Basin versus the Sorbas and Caltanissetta Basins cannot be uniquely disentangled. The offset can be attributed to either a change in the composition of basinal water (included in the calculation of x_2 in the mixing equation above), or variable resetting (f_{p2} above). The difference between the age-equivalent sub-basins (Sorbas and Caltanissetta) is interpreted as variable resetting, rather than differences in basinal water composition. Regardless, the composition of the initial sulfate reservoir is not directly preserved in these evaporite basins. Generally, this exercise explains how we expect basinal sulfate to evolve and identifies the dominate mechanisms at play in the isotopic resetting of the sulfate.

The natural extension of this argument is whether this degree of basinal sulfate resetting is realistic. Based on oxygen isotope arguments, we estimate that ~20% of evaporite sulfate in the Sorbas Basin (~30% for the Caltanissetta Basin) was re-equilibrated with evolved basin water. To loosely approximate the rates of biogeochemical sulfur cycling necessary to reset ~20% of the evaporite sulfate, we assume modern-like sulfate concentrations (28 mM) and basin geometry (surface area and volume). For this calculation we further assume that the Sorbas Basin gypsum was de-

posited approximately 1.29 million years after initial restriction of the Western Mediterranean Basin from the global ocean at 7.25 Ma (Roveri et al., 2014). These parameters yield an estimated requisite sulfate recycling flux of roughly ~7.5 mmol/m^2/yr. Setting aside sulfate contributions from other sources like sulfide oxidation (which would have implications for the requisite recycling flux), the sulfate regeneration flux via microbial sulfate reduction (J_{bio}) can be expressed as a function of net sulfate reduction (J_{SR}, and where $J_{SR} = F_{SO3} \cdot J_{bio}$). Here, the term F_{SO3} is the sulfate recycling efficiency and can vary between 0.1 to 10 across a range of typical cell specific sulfate reduction rates (Waldeck et al., 2019; Bertran et al., 2020). Thus, our prediction for the necessary net sulfate reduction activity needed to reset 20% of the sulfate in the Sorbas Basin observation is between 0.75 to 75 mmol/m^2/yr), which is in agreement with predictions from marine sediment pore waters over a range of water depths (Turchyn et al., 2006, and references therein).

6. Conclusions

As an atmospheric proxy, sulfate $\Delta'^{17}O$ is still in its infancy. This isotope proxy serves as one of the most quantitative means of accessing information about ancient pO_2/pCO_2 and GPP (Crockford et al., 2018). However, further exploration of the details and complexities of this isotope system will allow for better constraints on environmental change. While other studies have recently called into question the process by which atmospheric information is transferred to the marine sulfate pool (Waldeck et al., 2019; Hemingway et al., 2020), we focus our efforts here to understand the extent to which marine sulfate evaporite deposits accurately reflect the composition of contemporaneous, open marine sulfate.

Our detailed sampling of evaporites in the Western Mediterranean Basin provides greater resolution on the spatial and temporal variability in the oxygen isotope composition of sulfate within a marine evaporite basin. When viewed individually, the sampled evaporite sub-basins are normally distributed in $\delta^{18}O$ and $\Delta'^{17}O$, reflecting a well-mixed basinal sulfate pool on timescales of evaporite deposition. We interpret the sulfate to reflect both initial seawater sulfate composition of the ocean and contributions from post basin enclosure isotopic resetting. For this later point, it is difficult to uniquely identify the process(es) responsible for isotopic resetting, other than to say they carry some combination of mass-dependence, or more likely a relationship to the composition of evolving basinal waters.

Many of the considerations explored in the Messinian case study are applicable deeper in the geological record. Foremost is the observation that, despite a small isotopic offset in $\Delta'^{17}O$, sulfate evaporites still carry a strong memory of seawater sulfate. Conversely, the $\delta^{18}O$ of those same evaporites is more variable and is perhaps a better indicator of changes in basinal water budgets. This observation is consistent with the $\delta^{18}O$ of sulfate being a powerful proxy for differentiating marine and terrestrial evaporites, where other geological determinants are inconclusive. Finally, these arguments and our understanding of how the isotopic composition of basinal sulfate evolves benefit from attention to the distribution of data within a stratigraphic unit. Direct applications of these approaches deeper in time are complicated by variability in the $\delta^{18}O$ and $\Delta'^{17}O$ composition of atmospheric oxidants, the isotopic composition of seawater itself, and the requisite degree of supersaturation (a function of $[SO_4^{2-}]$). However, the mechanics of sulfate isotopic evolution within a marine evaporite basin are likely shared through time. It is with this final point that we offer a Messinian case study as a guide for geological reconstructions to come.

CRediT authorship contribution statement

Anna R. Waldeck: Conceptualization, Data curation, Methodology, Software, Visualization, Writing – original draft. **Haley C. Olson:** Conceptualization, Data curation, Methodology, Software, Visualization, Writing – original draft. **Weiqi Yao:** Methodology, Writing – review & editing. **Clara L. Blättler:** Resources, Supervision, Writing – review & editing. **Adina Paytan:** Funding acquisition, Resources, Writing – review & editing. **David A. Hodell:** Resources, Supervision, Writing – review & editing. **David T. Johnston:** Conceptualization, Funding acquisition, Methodology, Supervision, Writing – original draft.

Declaration of competing interest

The authors declare that they have no known competing financial interests or personal relationships that could have appeared to influence the work reported in this paper.

Acknowledgements

We thank two anonymous reviewers and the editor for insightful comments that improved the manuscript. Additionally we thank Lou Derry, Jordon Hemingway, Peter Crockford, Satish Iyengar, and members of the Johnston group for detailed feedback and discussions which improved the manuscript. Funding for this work was provided by Harvard University (H.O.), NSF OCE-1821958 and NSF OCE-1946137 (D.J.), NSF OCE-1946153 and NSF OCE-1821976 (A.P.), and European Research Council Grant 339694 (D.H.).

Appendix A. Supplementary material

Supplementary material related to this article can be found online at https://doi.org/10.1016/j.epsl.2021.117320.

References

Balci, N., Shanks III, W.C., Mayer, B., Mandernack, K.W., 2007. Oxygen and sulfur isotope systematics of sulfate produced by bacterial and abiotic oxidation of pyrite. Geochim. Cosmochim. Acta 71, 3796–3811.

Bao, H., 2015. Sulfate: a time capsule for Earth's O_2, O_3, and H_2O. Chem. Geol. 395, 108–118.

Bao, H., Lyons, J., Zhou, C., 2008. Triple oxygen isotope evidence for elevated CO_2 levels after a Neoproterozoic glaciation. Nature 453, 504–506.

Bao, H., Fairchild, I.J., Wynn, P.M., Spötl, C., 2009. Stretching the envelope of past surface environments: Neoproterozoic glacial lakes from Svalbard. Science 323, 119–122.

Bao, H., Chen, Z.-Q., Zhou, C., 2012. An ^{17}O record of late Neoproterozoic glaciation in the Kimberley region, Western Australia. Precambrian Res. 216, 152–161.

Berner, R.A., 2006. GEOCARBSULF: a combined model for Phanerozoic atmospheric O_2 and CO_2. Geochim. Cosmochim. Acta 70, 5653–5664.

Bertran, E., Waldeck, A., Wing, B., Halevy, I., Leavitt, W., Bradley, A., Johnston, D., 2020. Oxygen isotope effects during microbial sulfate reduction: applications to sediment cell abundances. ISME J. 14, 1508–1519.

Bishop, J.K., 1988. The barite-opal-organic carbon association in oceanic particulate matter. Nature 332, 341–343.

Brand, W.A., Coplen, T.B., Aerts-Bijma, A.T., Böhlke, J., Gehre, M., Geilmann, H., Gröning, M., Jansen, H.G., Meijer, H.A., Mroczkowski, S.J., et al., 2009. Comprehensive inter-laboratory calibration of reference materials for δ18O versus VSMOW using various on-line high-temperature conversion techniques. Rapid Commun. Mass Spectrom. 23, 999–1019.

Breit, G.N., Simmons, E., Goldhaber, M., 1985. Dissolution of barite for the analysis of strontium isotopes and other chemical and isotopic variations using aqueous sodium carbonate. Chem. Geol., Isot. Geosci. Sect. 52, 333–336.

Brunner, B., Bernasconi, S.M., Kleikemper, J., Schroth, M.H., 2005. A model for oxygen and sulfur isotope fractionation in sulfate during bacterial sulfate reduction processes. Geochim. Cosmochim. Acta 69, 4773–4785.

Cao, X., Bao, H., 2021. Small triple oxygen isotope variations in sulfate: mechanisms and applications. Rev. Mineral. Geochem. 86, 463–488.

Claypool, G.E., Holser, W.T., Kaplan, I.R., Sakai, H., Zak, I., 1980. The age curves of sulfur and oxygen isotopes in marine sulfate and their mutual interpretation. Chem. Geol. 28, 199–260.

Cowie, B.R., Johnston, D.T., 2016. High-precision measurement and standard calibration of triple oxygen isotopic compositions ($\delta^{18}O$, $\Delta'^{17}O$) of sulfate by F_2 laser fluorination. Chem. Geol. 440, 50–59.
Crockford, P.W., Hayles, J.A., Bao, H., Planavsky, N.J., Bekker, A., Fralick, P.W., Halverson, G.P., Bui, T.H., Peng, Y., Wing, B.A., 2018. Triple oxygen isotope evidence for limited mid-Proterozoic primary productivity. Nature 559, 613–616.
Crockford, P.W., Kunzmann, M., Bekker, A., Hayles, J., Bao, H., Halverson, G.P., Peng, Y., Bui, T.H., Cox, G.M., Gibson, T.M., et al., 2019. Claypool continued: extending the isotopic record of sedimentary sulfate. Chem. Geol. 513, 200–225.
Evans, D.A., 2006. Proterozoic low orbital obliquity and axial-dipolar geomagnetic field from evaporite palaeolatitudes. Nature 444, 51–55.
Evans, N.P., Turchyn, A.V., Gázquez, F., Bontognali, T.R., Chapman, H.J., Hodell, D.A., 2015. Coupled measurements of δ18O and δD of hydration water and salinity of fluid inclusions in gypsum from the Messinian Yesares Member, Sorbas Basin (SE Spain). Earth Planet. Sci. Lett. 430, 499–510.
Fritz, P., Basharmal, G., Drimmie, R., Ibsen, J., Qureshi, R., 1989. Oxygen isotope exchange between sulphate and water during bacterial reduction of sulphate. Chem. Geol., Isot. Geosci. Sect. 79, 99–105.
Gargani, J., Rigollet, C., 2007. Mediterranean Sea level variations during the Messinian salinity crisis. Geophys. Res. Lett. 34, L10405.
Gradstein, F.M., Ogg, J.G., Schmitz, M.D., Ogg, G.M., 2020. The Geologic Time Scale 2020. Elsevier.
Griffith, E.M., Paytan, A., 2012. Barite in the ocean–occurrence, geochemistry and palaeoceanographic applications. Sedimentology 59, 1817–1835.
Grossman, E., Joachimski, M., 2020. Chapter 10 - Oxygen isotope stratigraphy. In: Geologic Time Scale 2020. Elsevier B.V., pp. 279–307.
Hemingway, J.D., Olson, H., Turchyn, A.V., Tipper, E.T., Bickle, M.J., Johnston, D.T., 2020. Triple oxygen isotope insight into terrestrial pyrite oxidation. Proc. Natl. Acad. Sci. USA 117, 7650–7657.
Hodgskiss, M.S., Crockford, P.W., Peng, Y., Wing, B.A., Horner, T.J., 2019. A productivity collapse to end Earth's Great Oxidation. Proc. Natl. Acad. Sci. USA 116, 17207–17212.
Hsü, K.J., Ryan, W.B., Cita, M.B., 1973. Late Miocene desiccation of the Mediterranean. Nature 242, 240–244.
Johnston, D.T., Gill, B.C., Masterson, A., Beirne, E., Casciotti, K.L., Knapp, A.N., Berelson, W., 2014. Placing an upper limit on cryptic marine sulphur cycling. Nature 513, 530–533.
Killingsworth, B.A., Hayles, J.A., Zhou, C., Bao, H., 2013. Sedimentary constraints on the duration of the Marinoan Oxygen-17 Depletion (MOSD) event. Proc. Natl. Acad. Sci. USA 110, 17686–17690.
Knoll, A.H., 2011. The multiple origins of complex multicellularity. Annu. Rev. Earth Planet. Sci. 39, 217–239.
Knoll, A.H., Sperling, E.A., 2014. Oxygen and animals in Earth history. Proc. Natl. Acad. Sci. USA 111, 3907–3908.
Kohl, I., Bao, H., 2011. Triple-oxygen-isotope determination of molecular oxygen incorporation in sulfate produced during abiotic pyrite oxidation (pH = 2–11). Geochim. Cosmochim. Acta 75, 1785–1798.
Krijgsman, W., Hilgen, F.J., Raffi, I., Sierro, F.J., Wilson, D.S., 1999. Chronology, causes and progression of the Messinian salinity crisis. Nature 400, 652–655.
Krijgsman, W., Fortuin, A.R., Hilgen, F.J., Sierro, F.J., 2001. Astrochronology for the Messinian Sorbas basin (SE Spain) and orbital (precessional) forcing for evaporite cyclicity. Sediment. Geol. 140, 43–60.
Lazarus, D., 1994. Neptune: a marine micropaleontology database. Math. Geol. 26, 817–832.
Le Gendre, E., Martin, E., Villemant, B., Cartigny, P., Assayag, N., 2017. A simple and reliable anion-exchange resin method for sulfate extraction and purification suitable for multiple O- and S-isotope measurements. Rapid Commun. Mass Spectrom. 31, 137–144.
Markovic, S., Paytan, A., Li, H., Wortmann, U.G., 2016. A revised seawater sulfate oxygen isotope record for the last 4 Myr. Geochim. Cosmochim. Acta 175, 239–251.
Mayer, L., Pisias, N.G., Janecek, T.R., et al., 1992. In: Proceedings of the Ocean Drilling Program, Initial Reports, vol. 138, p. 1462.
Palmer, M.R., Helvací, C., Fallick, A.E., 2004. Sulphur, sulphate oxygen and strontium isotope composition of Cenozoic Turkish evaporites. Chem. Geol. 209, 341–356.
Passey, B.H., Levin, N.E., 2021. Triple oxygen isotopes in meteoric waters, carbonates, and biological apatites: implications for continental paleoclimate reconstruction. Rev. Mineral. Geochem. 86, 429–462.
Paytan, A., Griffith, E.M., 2007. Marine barite: Recorder of variations in ocean export productivity. Deep-Sea Res., Part 2, Top. Stud. Oceanogr. 54, 687–705.
Paytan, A., Kastner, M., Martin, E., Macdougall, J., Herbert, T., 1993. Marine barite as a monitor of seawater strontium isotope composition. Nature 366, 445–449.
Paytan, A., Kastner, M., Campbell, D., Thiemens, M.H., 1998. Sulfur isotopic composition of Cenozoic seawater sulfate. Science 282, 1459–1462.
Paytan, A., Kastner, M., Campbell, D., Thiemens, M.H., 2004. Seawater sulfur isotope fluctuations in the cretaceous. Science 304, 1663–1665.
Peng, Y., Bao, H., Zhou, C., Yuan, X., 2011. 17O-depleted barite from two Marinoan cap dolostone sections, South China. Earth Planet. Sci. Lett. 305, 21–31.
Razali, N.M., Wah, Y.B., et al., 2011. Power comparisons of Shapiro-Wilk, Kolmogorov-Smirnov, Lilliefors and Anderson-Darling tests. J. Stat. Model. Anal. 2, 21–33.
Reinhard, C.T., Planavsky, N.J., Olson, S.L., Lyons, T.W., Erwin, D.H., 2016. Earth's oxygen cycle and the evolution of animal life. Proc. Natl. Acad. Sci. USA 113, 8933–8938.
Renaudie, J., Lazarus, D., Diver, P., 2020. NSB (Neptune sandbox Berlin): an expanded and improved database of marine planktonic microfossil data and deep-sea stratigraphy. Palaeontol. Electronica 23, a11.
Roveri, M., Flecker, R., Krijgsman, W., Lofi, J., Lugli, S., Manzi, V., Sierro, F.J., Bertini, A., Camerlenghi, A., De Lange, G., et al., 2014. The Messinian Salinity Crisis: past and future of a great challenge for marine sciences. Mar. Geol. 352, 25–58.
Royer, D.L., Berner, R.A., Park, J., 2007. Climate sensitivity constrained by CO2 concentrations over the past 420 million years. Nature 446, 530–532.
Sharp, Z., Wostbrock, J., Pack, A., 2018. Mass-dependent triple oxygen isotope variations in terrestrial materials. Geochem. Perspect. Lett. 7, 27–31.
Spencer-Cervato, C., 1999. The Cenozoic deep sea microfossil record: explorations of the DSDP/ODP sample set using the Neptune database. Palaeontol. Electronica 2, 270.
Stefano, L., Vinicio, M., Marco, R., Charlotte, S.B., 2010. The Primary Lower Gypsum in the Mediterranean: a new facies interpretation for the first stage of the Messinian salinity crisis. Palaeogeogr. Palaeoclimatol. Palaeoecol. 297, 83–99.
Turchyn, A., Sivan, O., Schrag, D., 2006. Oxygen isotopic composition of sulfate in deep sea pore fluid: evidence for rapid sulfur cycling. Geobiology 4, 191–201.
Turchyn, A.V., Schrag, D.P., 2004. Oxygen isotope constraints on the sulfur cycle over the past 10 million years. Science 303.
Turchyn, A.V., Schrag, D.P., 2006. Cenozoic evolution of the sulfur cycle: insight from oxygen isotopes in marine sulfate. Earth Planet. Sci. Lett. 241, 763–779.
Utrilla, R., Pierre, C., Orti, F., Pueyo, J.J., 1992. Oxygen and sulphur isotope compositions as indicators of the origin of mesozoic and Cenozoic evaporites from Spain. Chem. Geol. 102, 229–244.
Von Allmen, K., Böttcher, M.E., Samankassou, E., Nägler, T.F., 2010. Barium isotope fractionation in the global barium cycle: first evidence from barium minerals and precipitation experiments. Chem. Geol. 277, 70–77.
Waldeck, A., Cowie, B., Bertran, E., Wing, B., Halevy, I., Johnston, D., 2019. Deciphering the atmospheric signal in marine sulfate oxygen isotope composition. Earth Planet. Sci. Lett. 522, 12–19.
Warren, J.K., 2010. Evaporites through time: tectonic, climatic and eustatic controls in marine and nonmarine deposits. Earth-Sci. Rev. 98, 217–268.
Wostbrock, J.A., Cano, E.J., Sharp, Z.D., 2020. An internally consistent triple oxygen isotope calibration of standards for silicates, carbonates and air relative to VSMOW2 and SLAP2. Chem. Geol. 533, 119432.
Yan, Y., Bender, M.L., Brook, E.J., Clifford, H.M., Kemeny, P.C., Kurbatov, A.V., Mackay, S., Mayewski, P.A., Ng, J., Severinghaus, J.P., et al., 2019. Two-million-year-old snapshots of atmospheric gases from Antarctic ice. Nature 574, 663–666.
Zeebe, R.E., 2010. A new value for the stable oxygen isotope fractionation between dissolved sulfate ion and water. Geochim. Cosmochim. Acta 74, 818–828.